J|A|C|S
COMMUNICATIONS

Published on Web 03/06/2002

Triple-Quantum Magic Angle Spinning ^{27}Al NMR of Aluminum Hydroxides

Krishnan Damodaran,[†] Pattuparambil R. Rajamohanan,[†] Debojit Chakrabarty,*[,‡] Uday Shankar Racherla,*[,‡] Venkat Manohar, Christian Fernandez,[§] Jean-Paul Amoureux,*[,||] and Subramanian Ganapathy*[,†]

National Chemical Laboratory, Pune 411008, India, Unilever Research India, Mumbai 400 099, India, ISMRA/Université de Caen, 14050 Caen, Cedex, France and Université des Sciences et Technologies de Lille-59655 Villeneuve d'Ascq Cedex, France

Received June 25, 2001; Revised Manuscript Received January 3, 2002

The third most common element in earth's crust is aluminum, and in nature there exist four of the five known crystalline forms of hydroxides, namely, the two trihydroxides, gibbsite and nordstrandite, and the two oxyhydroxides, boehmite and diaspore.[1] Although the other aluminum hydroxide, bayerite (β-Al(OH)$_3$), does not occur freely in nature, it can be prepared synthetically, as are the two other most widely used members of the family, gibbsite (α-Al(OH)$_3$) and boehmite (α-AlOOH). For the other two members, namely nordstrandite and diaspore, no commercial use or large-scale synthesis has been reported. Irreversible dehydration of aluminum hydroxides produces a series of so-called "transition" aluminas in a well-defined dehydration sequence,[2] resulting in α-Al$_2$O$_3$ as the end member. Their thermal decomposition under controlled synthetic condition produces alumina-derived materials of desired morphology and texture. Thus, at the heart of industrial aluminas and ceramics lie these three starting materials of great fundamental importance. Aluminum hydroxides are different configurations of the same structure, the building block of which is the "Pauling Octahedra", where the octahedra are formed by Al−O and O−H bonds that impart stability to the compact structure.

As an adjunct to X-ray diffraction, high-resolution solid-state NMR is sought to differentiate between various crystalline configurations. ^{27}Al MAS NMR, often used to distinguish Al in different coordinations (tetra, penta, octahedral), is of no avail in the structural characterization of aluminum hydroxides since nonequivalent Al environments within a given coordination (octahedral) remain undetected. This is due to residual second-order quadrupolar broadening not altogether eliminated by MAS in the "central transition" ($-^1/_2$,$^1/_2$) dominated ^{27}Al spectra.[3] Consequently, it is not possible to study minor structural modifications involving small variations in the coordination geometry, as would occur in basic aluminum hydroxides and the thermally decomposed alumina forms.

The recent advent of multiple-quantum magic angle spinning (MQ-MAS) NMR[4] alleviates this problem. This experiment exploits the definite correlation of the orientation dependent frequencies, evolving during the multiple-quantum (3Q, 5Q for ^{27}Al) evolution period (t_1), with the corresponding single-quantum ($-^1/_2$,$^1/_2$) frequencies in the acquisition period (t_2). ^{27}Al isotropic spectra, devoid of second-order quadrupolar broadenings, are obtained after a shearing[4b] operation of MQ-MAS data, and they now facilitate inspection of nonequivalent Al environments within a given Al coordination. Further benefits of a high detection sensitivity ensue due to high ^{27}Al natural abundance (100%). We show in this communication that new opportunities are offered in the identification of Al environments in basic synthetic aluminum hydroxides, as a prelude to phase identification and quantification in various structurally transformed materials.

We show in Figure 1 the ^{1}H decoupled ^{27}Al 3Q-MAS NMR spectra of boehmite, bayerite, and gibbsite. Besides clearly depicting the presence of nonequivalent octahedral aluminum in the structure, 3Q-MAS spectra provide valuable data on the chemical shielding and electric field gradient parameters to further aid in the structural distinction. In gibbsite[5,6] and bayerite, consistent with their structures, we detect two ^{27}Al isotropic resonances with a 1:1 intensity from triple-quantum experiments.[7] A graphical analysis[8] of 3Q-MAS contour plots (Figure 1) provides isotropic chemical shifts (δ_{cs}) and quadrupole interaction parameters (P_Q), while 1D MAS simulations, shown in Figure 1C, yield the values of η_Q and further confirm the 1:1 intensity ratio for the two aluminum trihydroxide polymorphs. Values of all the experimentally determined parameters are included in Table 1.

There are two crystallographically inequivalent aluminums that build layers of edge-sharing Al(OH)$_6$ octahedra (called A and B), to produce the stacked layer sequence AB BA AB... (gibbsite)[9] and AB AB AB... (bayerite)[10] (Figure 1A). In bayerite, hydroxyl groups of one layer lie in the depressions between the hydroxyls in the second, while in gibbsite, the hydroxyls of the adjacent layers are situated directly opposite each other, causing the layers to be displaced along *a*-axis. The two distinct octahedral environments in bayerite and gibbsite show striking dissimilarity in the way chemical shielding and quadrupole interaction parameters are affected by the difference in the stacking sequence. In gibbsite, the two Al sites show a larger difference in P_Q than in δ_{cs}. In bayerite, this is reversed. The enhanced peak resolution for the isotropic resonances in gibbsite is due to a large positive quadrupole-induced shift for one of the sites (Al2) along the sheared triple-quantum dimension. Despite the relatively large quadrupole interaction, this site is equally as well excited as the other Al site so that ($0Q \rightarrow \pm 3Q$) creation and ($\pm 3Q \rightarrow 0Q$) conversion efficiencies are nearly equal. These are supported by density matrix calculations,[11] using δ_{cs} and P_Q values determined by graphical analysis and ν_{rf} (60 kHz) used in the experiment. While trying to assign the isotropic resonances obtained from 3Q-MAS experiments to the inequivalent octahedra in the structure, we find that correlations[12] based on (T−O−T)/(O−T−O) with δ_{cs}/P_Q do not lead to unambiguous assignments for the isotropic resonances since the large difference in e^2qQ/h (2.5 MHz) (gibbsite) or δ_{cs} (~4 ppm) (bayerite) is not accounted for by the smaller differences in octahedral distortion derived from an analysis of O−T−O or T−O−T angles. For signal assignments, independent ab initio calculations[13] of electric field gradient tensors, were carried out by us for gibbsite

* Corresponding author. E-mail: ganpat@ems.ncl.res.in. Fax: 91-20-5893234.
[†] National Chemical Laboratory.
[‡] Unilever Research India.
[§] University of Caen.
[||] University of Lille.

10.1021/ja011532y CCC: $22.00

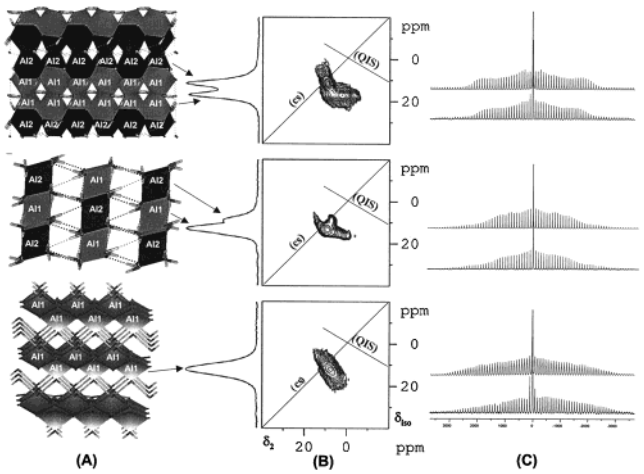

Figure 1. The identification of crystallographically nonequivalent aluminum octahedra, in the structures (**A**) of boehmite (bottom), bayerite (middle), and gibbsite (top) from the 2D contour plots of ^{27}Al triple-quantum MAS NMR experiments (**B**). The assignments of ^{27}Al isotropic peaks appearing along ω_{iso} axis are shown. The δ_{cs} (slope 1) and δ_{QIS} (slope $-10/17$) axes are marked in the 2D contour plot, and these aid in the graphical analysis of the 3Q-MAS data. Spectra in (**C**) are experimentally obtained 1D ^{27}Al MAS spectra, shown to depict the satellite sideband patterns (bottom spectra in each case), which are successfully simulated (top spectra in each case) using the values given in Table 1. Rotor-synchronized ((ν_r = 13 kHz) ^{1}H decoupled (TPPM[19] decoupling) *z*-filter[20] 3Q-MAS experiments were performed at 130.318 MHz on a Bruker DRX-500 FT-NMR spectrometer (128 t_1 increments (76.92 μs) and 480 scans. The 1024 × 1024 2D data matrix was apodized using an exponential (LB = 10 Hz) (gibbsite and boehmite) or sine-squared bell (SSB = 8) (bayerite) window functions along t_1 prior to Fourier transformation and shearing.

Table 1. Chemical Shift and Quadrupole Interaction Parameters of Aluminum Hydroxides

aluminum hydroxide	δ_{iso} (ppm)	δ_{cs}	$(e^2qQ/h)^a$ MHz	$\eta_Q{}^a$	assignment
gibbsite	11.6	10.5 ± 0.2	2.2 ± 0.2 (2.2, 2.6)	0.75 ± 0.05 (1.0,1.0)	Al (2)
	17.2	11.5 ± 0.2	4.7 ± 0.2 (3.2, 3.9)	1.00 ± 0.05 (0.57,0.40)	Al (1)
bayerite	9.1	8.3 ± 0.2	1.9 ± 0.1 (2.5, 3.0)	0.25 ± 0.05 (0.72,0.70)	Al (2)
	13.1	12.4 ± 0.2	1.4 ± 0.1 (1.4, 1.6)	0.80 ± 0.05 (0.58,0.90)	Al (1)
boehmite	12.6	11.0 ± 0.5	1.8−2.8	0.5−1.0	Al (1)

[a] $(e^2qQ/h) = P_Q(1 + \eta_Q{}^2/3)^{-1/2}$ (P_Q from graphical analysis). η_Q determined by simulation of 1D MAS spectra. For boehmite, 1D MAS simulation required a distribution of e^2qQ/h and η_Q values in the range indicated. Values in parentheses are the e^2qQ/h and η_Q determined from ab initio calculations using small (HF/6-31g(d,p)) and large (HF/6-311++g(2d,2p)) basis sets. Errors in the experimentally determined values of δ_{ISO}, e^2qQ/h and η_Q were estimated from analysis of 1D MAS spectra.

and bayerite using different basis sets and clusters (tetramer, decamer) built from crystal structure data.[9,10] Calculated values of e^2qQ/h, which are more reliable than η_Q,[14,15] show convergence and a trend analogous to that noticed in the experimentally determined values of e^2qQ/h (Table 1). This leads to the unambiguous assignment of the two nonequivalent octahedra in the structures of gibbsite and bayerite and is shown in Figure 1. The oxyhydroxide polymorph boehmite (AlOOH) displays a single but broad (∼5 ppm) isotropic resonance. In the structure of boehmite, equivalent aluminum octahedra are formed by coordination of Al to nonequivalent oxygens,[16] and these octahedra are set out in straight double chains to build a sheetlike structure (Figure 1A) linked through hydrogen bonds between hydroxyls in neighboring planes. The lack of high resolution may be traced to disorder in Al positions in the crystal,[17] leading to small variations in the isotropic chemical shift and quadrupolar couplings. The larger line width for the isotropic signal of boehmite is entirely consistent with the somewhat poor crystallinity observed in XRD pattern. The elongation of the 2D contour parallel to the QIS direction shows that the observed broadening is dictated by a distribution of quadrupole couplings and to a smaller degree by chemical shift dispersion. Boehmite is known to exhibit a distribution of water content and crystallite size.[18]

In conclusion, the structural distinction of the aluminum hydroxides has been made through identification, quantification, and unambiguous assignment of the structure building octahedral aluminum environments through 3Q-MAS experiments and ab initio quantum chemical calculations. Our findings pave the way for future studies on the phase identification and quantification in various structurally transformed materials.

Acknowledgment. We thank IFCPAR, New Delhi, and HLRC, Mumbai, for financial support. We thank Dr. Sourav Pal for valuable discussions regarding calculations of EFG tensors and Miss Raina Gupta for experimental assistance. J.P.A. thanks the Region Nord/Pas de Calais for strong support.

Supporting Information Available: Structure data, FT-IR and XRD spectra; ab initio EFG and chemical shielding tensor calculation results and density matrix calculations (PDF). This material is available free of charge via the Internet at http://pubs.acs.org.

References

(1) *Alumina as a Ceramic Material*; Gitzen, W. H., Ed.; American Ceramic Society: Columbus, OH, 1970.
(2) Wefers, K.; Misra, C. *Alcoa Technical Paper No. 19*; Alcoa Laboratories: Pittsburgh, PA, 1987.
(3) Freude, D. *Encyclopedia of Analytical Chemistry*; Meyers, R. A., Ed.; 2000; pp 12188−12224.
(4) (a) Frydman, L.; Harwood, J. S. *J. Am. Chem. Soc.* **1995**, *117*, 5367−5368. (b) Medek, A.; Harwood, J. S.; Frydman, L. *J. Am. Chem. Soc.* **1995**, *117*, 12779−12787.
(5) Ashbrook, S. E.; McManus, J.; Mackenzie, K. J. D.; Wimperis, S. *J. Phys. Chem. B* **2000**, *104*, 6408.
(6) McManus, J.; Ashbrook, S. E.; Mackenzie, K. J. D.; Wimperis, S. *J. Non-Cryst. Solids* **2001**, *282*, 278−290.
(7) For bayerite, the intensity ratio of 1:1 for the two nonequivalent octahedral Al environments was verified in the 2D data processed without resolution enhancement, followed by spectral deconvolution.
(8) Fernandez, C.; Amoureux, J. P.; Chezeau, J. M.; Delmotte, L.; Kessler, H. *Microporous Mesoporous Mater.* **1996**, *6*, 331.
(9) Saalfeld, H.; Wedde, M. *Z. Kristallogr.* **1974**, *139*, 129−135.
(10) Zigan, F.; Joswig, W.; Burger, N. *Z. Kristallogr.* **1978**, *148*, 255−273.
(11) (a) Amoureux, J. P.; Fernandez, C.; Dumazy, Y. *J. Chim. Phys.* **1995**, *2*, 1939. (b) Bak, M.; Rasmussen, T.; Nielsen, N. Chr. *J. Magn. Reson.* **2000**, *147*, 296−330.
(12) (a) Delaye, J. M.; Charpentier, T.; Petit, J. C.; Ghaleb, D.; Faucon, P. *Chem. Phys. Lett.* **2000**, *320*, 681. (b) Hunger, H.; Horvath, T. *J. Am. Chem. Soc.* **1996**, *118*, 12302.
(13) The ab initio calculations were carried out using the Gaussian 98 program installed on an IBM RS6000/SP3 cluster for the calculation of electric field gradient and chemical shielding tensors.
(14) Since $\eta_Q = |(q_{xx} - q_{yy})/q_{zz}|$ and $C_Q = e^2qQ/h = eQ{\cdot}eq_{zz}$, the error propagation, due to uncertainty in the calculated values of the diagonal elements of the electric field gradient tensor, leads to larger errors for η_Q than for C_Q. The level of theory and the choice of basis sets and cluster size we have used represent an acceptable compromise between precision and computational speed and ensure that the calculated values of C_Q converge as basis sets increase. Thus, the isotropic ^{27}Al resonances of gibbsite and bayerite could be assigned based on the calculations of C_Q parameter alone.
(15) (a) Torrent, M.; Musaev, D. G.; Morokuma, K. *J. Phys. Chem. B* **1999**, *103*, 8618−8627. (b) Murgich, J.; Aray, Y.; Soscum, H. J.; Marino, R. A. *J. Phys. Chem.* **1992**, *96*, 9198.
(16) Walter, T. H.; Oldfield, E. *J. Phys. Chem.* **1989**, *93*, 6744.
(17) Hill, R. J. *Clays Clay Miner.* **1981**, *29*, 435−445.
(18) (a) Tettenhorst, R.; Hofmann, D. A.*Clays Clay Miner.* **1980**, *28*, 373−380. (b) Papee, D.; Tertian, R.; Biais, R. *Bull. Soc. Chim. Fr. Mem. Ser.* **1958**, *5*, 1301−1310.
(19) Bennet, A. E.; Rienstra, C. M.; Auger, M.; Lakshmi, K. V.; Griffin, R. G. *J. Chem. Phys.* **1995**, *103*, 6951.
(20) Amoureux, J. P.; Fernandez, C.; Steuernagel, S. *J. Magn. Reson., Ser. A* **1996**, *123*, 116.

JA011532Y